The Multidrug Resistance Protein Is Photoaffinity Labeled by a Quinoline-Based Drug at Multiple Sites†

Roni Daoud,‡ Jose Desneves,§ Leslie W. Deady,§ Leann Tilley,§ Rik J. Scheper,|| Philippe Gros,⊥ and Elias Georges*,‡

Institute of Parasitology, Department of Biochemistry, McGill University, Macdonald Campus, Ste-Anne de Bellevue, Quebec, Canada, The School of Chemistry and The School of Biochemistry, La Trobe University, Bundoora, Victoria, Australia, and Department of Pathology, Free University Hospital, Amsterdam, The Netherlands

Received September 23, 1999; Revised Manuscript Received December 28, 1999

ABSTRACT: Tumor cells overcome cytotoxic drug pressure by the overexpression of either or both transmembrane proteins, the P-glycoprotein (P-gp) and the multidrug resistance protein (MRP). The MRP has been shown to mediate the transport of cytotoxic natural products, in addition to glutathione-, glucuronidate-, and sulfate-conjugated cell metabolites. However, the mechanism of MRP drug binding and transport is at present not clear. In this study, we have used a photoreactive quinoline-based drug, *N*-(hydrocinchonidin-8′-yl)-4-azido-2-hydroxybenzamide (IACI), to show the photoaffinity labeling of the 190 kDa protein in membranes from the drug resistant SCLC H69/AR cells. The photoaffinity labeling of the 190 kDa protein by IACI was saturable and specific. The identity of the IACI-photolabeled protein as the MRP was confirmed by immunoprecipitation with the monoclonal antibody QCRL-1. Furthermore, a molar excess of leukotriene C_4, doxorubicin, colchicine, and other quinoline-based drugs, including MK571, inhibited the photoaffinity labeling of the MRP. Drug transport studies showed lower IACI accumulation in MRP-expressing cells which was reversed by depleting ATP levels in H69/AR cells. Mild digestion of the purified IACI-photolabeled MRP with trypsin showed two large polypeptides (∼111 and ∼85 kDa). The 85 kDa polypeptide which contains the QCRL-1 and MRPm6 monoclonal antibody epitopes corresponds to the C-terminal half of the MRP (amino acids ∼900−1531) containing the third multiple spanning domain (MSD3) and the second nucleotide binding site. The 111 kDa polypeptide which contains the epitope sequence of the MRPr1 monoclonal antibody encodes the remainder of the MRP sequence (amino acids 1−900) containing the MSD1 and MSD2 plus the first nucleotide binding domain. Cleveland maps of purified IACI-labeled 85 and 111 kDa polypeptides revealed 6 kDa and ∼6 plus 4 kDa photolabeled peptides, respectively. In addition, resolution of the exhaustively digested IACI-photolabeled MRP by HPLC showed two major and one minor radiolabeled peaks that eluted late in the gradient (60 to 72% acetonitrile). Taken together, the results of this study show direct binding of IACI to the MRP at physiologically relevant sites. Moreover, IACI photolabels three small peptides which localize to the N- and C-halves of the MRP. Finally, IACI provides a sensitive and specific probe for studying MRP−drug interactions.

Treatment of cancer patients with chemotherapeutic drugs is often unsuccessful due to the emergence of drug resistant tumors. Similarly, tumor cell lines selected in vitro with anticancer drugs become resistant to multiple drugs with concurrent overexpression of either or both transmembrane proteins, the P-glycoprotein (P-gp1)[1] and the multidrug resistance protein (MRP) (*1*−*3*). Gene transfer studies with human P-gp1 or MRP cDNA were shown to confer resistance to similar anticancer drugs onto previously drug susceptible cells (*4*, *5*). Furthermore, disruption of P-gp1 or MRP genes in mice led to increased sensitivity to natural product toxins and elevated glutathione levels in MRP-expressing tissues (*6*−*8*). Although both proteins are likely to mediate several physiological functions, P-gp1 appears to function as a nonspecific efflux pump at the blood−brain barrier (*6*), while MRP functions include mediation of inflammatory responses (*8*). Moreover, both proteins have been shown to function as "flipases" of short chain lipids (*9*, *10*) and to mediate the transport of normal cell metabolites and xenobiotics (*5*, *11*−*13*).

P-gp1 and the MRP are members of a large family of membrane-trafficking proteins that couple ATP hydrolysis to ligand transport across the cell membrane (*14*); however, the amino acid sequences of the two proteins are 15% identical (*15*). MRP primary structure encodes an MDR-like core of two membrane-spanning domains (MSD2 and

† This work was supported by grants from the Natural Sciences and Engineering Research Council of Canada to E.G. Research at the Institute of Parasitology is partially supported by a grant from the FCAR pour l'aide à la recherche.

* To whom correspondence should be addressed: Institute of Parasitology, McGill University, 21, 111 Lakeshore Road, Ste-Anne de Bellevue, PQ H9X 3V9. Telephone: (514) 398-8137. Fax: (514) 398-7857. E-mail: Elias_Georges@maclan.McGill.CA.

‡ Institute of Parasitology, McGill University.

§ La Trobe University.

|| Free University Hospital.

⊥ Department of Biochemistry, McGill University.

[1] Abbreviations: MDR, multidrug resistance; P-gp, P-glycoprotein; MRP, multidrug resistance protein; SCLC, small cell lung cancer; SDS−PAGE, sodium dodecyl sulfate−polyacrylamide gel electrophoresis; ABC, ATP binding cassette.

10.1021/bi9922188 CCC: $19.00
Published on Web 04/26/2000

MSD3) and two nucleotide-binding domains (NBD1 and NBD2), in addition to a 220-amino acid N-terminal membrane-spanning domain (MSD1) (*16*−*18*). Although the role of MSD1 remains to be clarified, it is thought to contain five transmembrane helices with an extracytosolic N-terminus (*17*, *18*). Furthermore, deletion of the first transmembrane helix from MSD1 or the entire MSD1 plus the linker sequence between MDS1 and MDS2 was shown to inhibit MRP-mediated transport of LTC_4 (*19*). More recently, Bakos et al. (*20*) showed that the deletion of all transmembrane helices of MSD1 had no effect on MRP-mediated LTC_4 transport. Interestingly, deletion of the linker domain between MSD1 and MSD2 abolished LTC_4 transport (*20*).

Several studies have shown MRP-mediated transport of glutathione-, glucuronidate-, and sulfate-conjugated drugs (*11*, *21*−*23*). The glutathione-conjugated eicosanoid, leukotriene C4 (LTC_4), is the highest-affinity substrate for MRP transporter (*11*, *21*, *22*). Indeed, the MRP appears to function as a cotransporter of glutathione; hence, MRP-like proteins are known as GS-X pumps or multispecific organic anion transporters (*24*, *25*). The ability of MRP to bind and transport unmodified drugs remains to be resolved. The MRP was shown to transport several unmodified drugs and natural products (*26*, *27*). For example, direct binding and transport of unmodified quinoline-based drugs in MRP-expressing MDR cells has been previously described (*27*−*29*). However, Loe et al. (*30*) found MRP-mediated active transport of unmodified vincristine only in the presence of GSH.

Photoreactive drug analogues have been previously employed to study protein receptor interactions with small ligand molecules (*31*). The use of photoreactive drug analogues that photoaffinity label P-gp has demonstrated the presence of at least two drug binding sites which map to sequences in transmembranes 5 and 6, and 11 and 12 (*32*). The drug binding domains identified by photoaffinity labeling were later confirmed by mutational analyses of P-gp1 TMs sequences (*33*). Several attempts to photoaffinity label the MRP with commercially available P-gp-specific photoreactive drugs have not been successful (*28*, *34*). Leier et al. (*11*) demonstrated the photoaffinity labeling of MRP with [^{3}H]LTC_4. The specificity of LTC_4 photoaffinity labeling was confirmed by competition experiments with nonradiolabeled LTC_4 and MK571, a quinoline-based antagonist of the LTD_4 receptor which reverses MRP-mediated MDR (*35*). However, photoaffinity labeling of MRP by [^{3}H]LTC_4 suffers from a weak photolabeling efficiency which limits its usefulness in studying MRP−drug interactions. Furthermore, with respect to MRP binding to anticancer drugs, it is not known if LTC_4 and unmodified anticancer drugs bind to the same sites. In this report, we demonstrate specific photoaffinity labeling of the MRP by a quinoline-based photoreactive drug. Moreover, our results show for the first time photoaffinity labeling of three sites in the N- and C-halves of the MRP.

MATERIALS AND METHODS

Materials. Iodine-125 (100.7 mCi/mL) was purchased from Amersham Biochemical Inc. (Mississauga, ON). Protein A-coupled Sepharose was purchased from Pharmacia Inc. (Montreal, PQ). The LTD_4 receptor antagonist MK571 was kindly provided by A. W. Ford-Hutchinson (Merck-Frost Centre for Therapeutic Research, Point Claire-Dorval, PQ; *36*). Leukotriene C_4 (LTC_4) was purchased from Cayman Chemical Co. (Ann Arbor, MI). The small cell lung cancer cells (H69 and H69/AR) and the MRP-specific monoclonal antibody (QCRL-1) were kind gifts from S. P. C. Cole (Cancer Research Laboratories, Queen's University, Kingston, ON). All other chemicals were of the highest commercial grade available.

Cell Culture and Plasma Membrane Preparations. Drug sensitive (H69) and resistant (H69/AR) cells were grown in RPMI 1640 medium containing 4 mM glutamine and 5% fetal calf serum (Hyclone). Resistant cells were cultured continuously in the presence of 0.8 μM doxorubicin; however, cells used for drug transport studies were grown in drug-free medium for 10 days prior to the date of the experiment. Plasma membranes from H69 and H69/AR cells were prepared as described by Lin et al. (*37*). In brief, cells were collected by low-speed centrifugation and washed three times with ice-cold phosphate-buffered saline (PBS) (pH 7.4). Cells were homogenized in 50 mM mannitol, 5 mM Hepes, and 10 mM Tris-HCl (pH 7.4) (containing 2 mM PMSF and 3 μg/mL leupeptin) in a Dounce glass homogenizer. A calcium chloride solution was then added to the homogenate to a final concentration of 10 mM and the solution mixed by stirring to ensure even distribution of the cation. The slightly turbid supernatant solution that contains plasmalemma vesicles was pelleted by high-speed centrifugation at 100000*g* for 1 h at 4 °C using a Beckman SW28 rotor. For sucrose gradient purification, the membrane suspension was adjusted to a final sucrose concentration of 45% with the addition of sucrose powder. The gradient was set up in 14 mL polycarbonate tubes using 1 mL of 60% sucrose, 5 mL of membranes in 45% sucrose, 2.5 mL of 35% sucrose, and 2.5 mL of 30% sucrose. Samples were spun for 3 h at 35 000 rpm and 4 °C. Membranes floating at the 30, 35, and 45% interfaces were harvested and washed with 10 mM Tris-HCl (pH 7.4). The enriched plasma membrane fraction was resuspended in the same buffer containing 250 mM sucrose. Membranes were stored at −80 °C if not immediately used. Protein concentrations were determined by the Lowry method (*38*).

Radioiodination and Photoaffinity Labeling. The coupling method used in the synthesis of photoreactive drugs (IACI) has been previously described elsewhere (*39*). Details of the synthesis will be described elsewhere. Iodination of IACI was carried out in the dark. Briefly, IACI (10 nmol) was dissolved in 20 μL of dimethyl sulfoxide (DMSO) and mixed with 10 μL of carrier-free Na^{125}I (1 mCi, 0.5 nmol) and 10 μL of chloramine T (10 nmol) in 1 M K_2HPO_4 (pH 7.4). The reaction was allowed to continue for 5 min and was stopped by the addition of sodium metabisulfite [50 μL of a 5% (w/v) solution]. The reaction mixture was loaded onto a C_{18} cartridge (Sep-Pak, Waters-Millipore) prewashed with 10 mM K_2HPO_4 (pH 7.4). The column was washed with 5 mL aliquots of 10 mM K_2HPO_4 (pH 7.4) containing 10% (v/v) methanol until no significant radiolabel was detected. IACI was eluted with 2.5 mL of methanol and vacuum-dried in the dark. The dried residue was resuspended in DMSO and the concentration of the radioactive, photoactive drug determined by HPLC.

Either plasma membranes (10−20 μg) or intact cells (5×10^6 cells) were photoaffinity labeled with IACI. Briefly, membranes or cells were photoaffinity labeled by IACI

(0.20−1.0 μM) in the absence or the presence of a molar excess of colchicine, chloroquine, doxorubicin, LTC_4, or MK571. Membranes or cells were incubated at room temperature in the dark for 30 min and then transferred to ice for 10 min. Following the latter incubation, cells were irradiated for 10 min on ice with a UV source at 254 nm (Stratagene UV cross-linker, Stratagene, La Jolla, CA). The free photoactive drug was removed by centrifugation, and cells were lysed in 20 μL of 50 mM Tris (pH 7.4) containing 1% Nonidet P-40 (NP40), 5 mM $MgCl_2$, and protease inhibitors (3 μg/mL leupeptin and 2 mM PMSF). Photoaffinity-labeled proteins were isolated by brief centrifugation at 4 °C and resolved on SDS−PAGE. It should be mentioned that incubation of cells or membranes with IACI but without UV irradiation did not result in the photoaffinity labeling of proteins (data not shown).

Immunoprecipitation and SDS Gel Electrophoresis. IACI photoaffinity-labeled cells were lysed in 50 mM Tris-HCl (pH 7.4) containing 0.5% CHAPS, 0.5% sodium deoxycholate, 150 mM NaCl, and protease inhibitors (3 μg/mL leupeptin and 2 mM PMSF). The cell lysates were clarified by centrifugation at 12000*g* and 4 °C. Equal amounts of cell lysate proteins were separately incubated overnight at 4 °C with 10 μg of QCRL-1, MRPr1, or MRPm6 monoclonal antibodies (Mabs) or an irrelevant IgG_{2a}. Protein A-coupled Sepharose was added to cell lysates and the mixture allowed to incubate for 1 h at room temperature. After several washes in lysis buffer, proteins were released from the Sepharose beads with buffer I [10 mM Tris-HCl (pH 8.0) containing 2% SDS, 50 mM dithiothreitol (DTT), and 1 mM ethylenediaminetetraacetate (EDTA)] and buffer II (2× buffer I and 9 M urea). Immunopurified proteins were eluted and resolved by SDS−PAGE using the Laemmli or Fairbanks gel system (*40*, *41*). Gel slabs containing the immunoprecipitated proteins were fixed in 50% methanol, dried, and exposed to XAR Kodak film at −70 °C for 2−12 h. Alternatively, proteins were visualized by silver staining, using the NOVEX SilverXpress Silver Staining Kit.

Proteolytic Digestion and HPLC. Immunopurified photoaffinity-labeled MRP bands were cut out of dried SDS−PAGE gels and digested with increasing concentrations of *Staphylococcus aureus* V8 protease (1−20 μg/gel slice) in the well of a 15% Laemmli gel (*41*) according to the method of Cleveland et al. (*42*). For partial digestion of the IACI photoaffinity-labeled MRP, 100 μg of H69 and H69/AR plasma membrane samples was photolabeled with 0.2 μM IACI and immunoprecipitated overnight with QCRL-1 Mab as previously described (*43*). Protein A-coupled Sepharose beads were washed in buffer A [0.1% TX-100, 0.03% SDS, 0.05 M Tris-HCl (pH 7.4), 5 mg/mL fraction V bovine serum albumin (BSA), and 150 mM NaCl] containing protease inhibitors (0.1 mM PMSF, 3 μg/mL leupeptin, pepstatin A, and aprotinin) followed by several washes without protease inhibitors. Mild trypsin digestion was carried out in the presence of 8 or 16 ng of trypsin at 37 °C for 5 min. Digestion was stopped with 10 μg/mL leupeptin, pepstatin A, aprotinin, and 1 mM PMSF followed by incubation for 5 min at 65 °C in SDS−PAGE sample buffer. Samples were resolved on Fairbanks gels, transferred to nitrocellulose membranes, and probed with QCRL-1, MRPm6, and MRPr1 monoclonal antibodies. Alternatively, partially digested fragments were immunoprecipitated separately with MRPr1 or MRPm6. Following an overnight immunoprecipitation, protein A-coupled Sepharose beads with MRP halves (85 and 111 kDa polypeptides) were washed and incubated with 40 μg of V8 protease in 50 mM Na_2HPO_4 (pH 7.4). Digestion was allowed to proceed for 16 h at 37 °C, and samples were then resolved on Fairbanks gels (*41*).

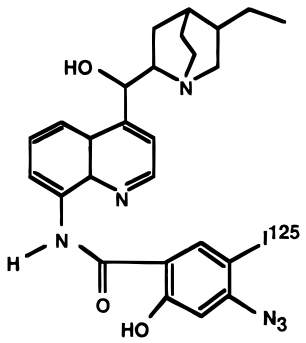

IACI

FIGURE 1: Organic structure of *N*-(hydrocinchonidin-8′-yl)-4-azido-2-hydroxybenzamide (IACI).

For a complete trypsin digestion, gel slices were rehydrated for 5 min in water prior to the elution of the IACI photoaffinity-labeled MRP, using the GE200 SixPacGel Eluter (Hoefer Scientific Instruments). The buffer of the eluted protein was changed to 50 mM ammonium bicarbonate (pH 8.0) by repeated washing using the Spin-X UF concentrators with a 100 000 kDa cutoff. The digestion commenced at 37 °C with the addition of 2 and 1 μg of trypsin for 14 and 4 h, respectively. The digested sample was vacuum-dried, resuspended in 250 μL of 1% trifluoroacetic acid in water, and resolved by reverse phase HPLC (Vydac 201HS54 C_{18} RP column). The chromatographic procedure consisted of an 80 min gradient of 0 to 100% acetonitrile with 1% trifluoroacetic acid at a flow rate of 1 mL/min. Fractions were collected and checked for radioactivity.

Drug Accumulation. Drug sensitive and resistant cells (1×10^6 cells) were washed three times with PBS (pH 7.4) and incubated at 37 °C with 10 mM D-glucose or 10 mM 2-deoxyglucose and 100 nM sodium azide. One micromole of IACI was added, and drug accumulation in cells was assessed in 0 and 60 min incubations as previously described (*44*).

RESULTS

Photoaffinity Labeling of the MRP with IACI. The MRP has been shown to mediate the transport of conjugated cell metabolites and natural product toxins (*22*, *23*, *45*). Several studies have now demonstrated a direct binding between one such glutathione-containing compound, cysteinyl leukotriene (LTC_4), and the MRP (*11*, *46*). However, MRP interaction with unmodified compounds remains unclear. In this study, we examined the photoaffinity labeling of plasma membrane proteins from a MRP-expressing cell line (H69/AR) by a photoactive quinoline-derived drug (IACI; Figure 1). To determine if IACI binds directly to the MRP, plasma membranes from drug sensitive (H69) and resistant (H69/AR) SCLC cells were incubated in the presence of 0.20 μM IACI and UV irradiated (see Materials and Methods). The results in Figure 2A show a 190 kDa protein photolabeled

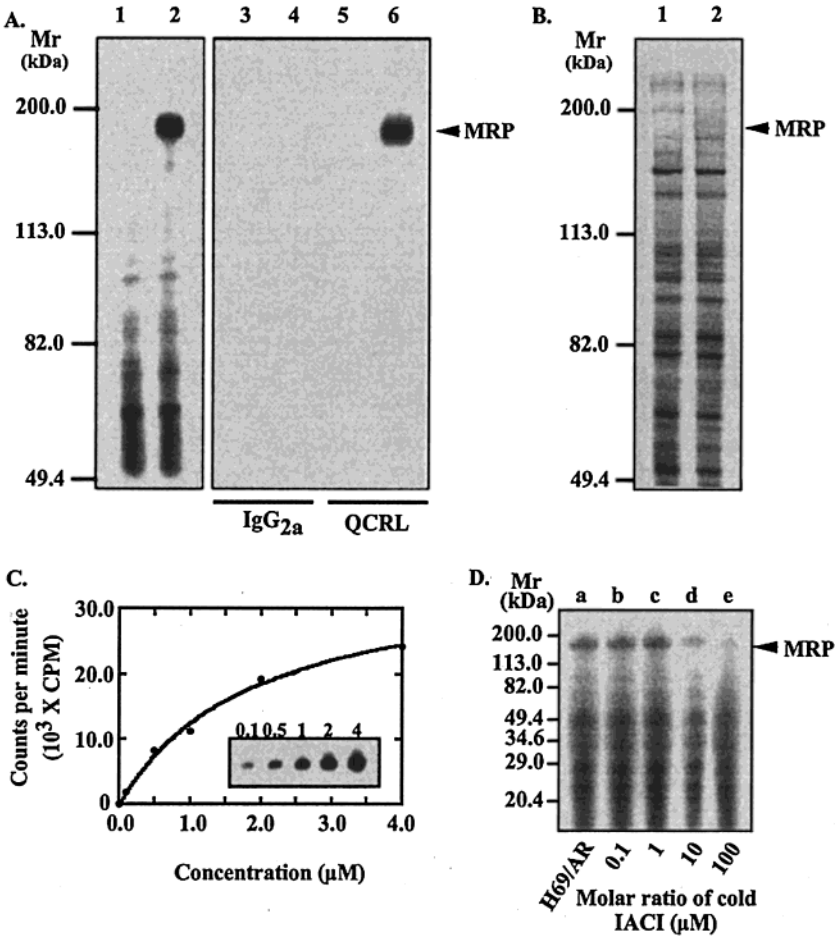

FIGURE 2: Photoaffinity labeling of MRP by IACI. Plasma membranes from drug sensitive (H69) and resistant (H69/AR) cells were photoaffinity labeled with 0.20 μM IACI and resolved on SDS−PAGE (A). Panel A also shows IACI photoaffinity-labeled membranes from H69 and H69/AR cells immunoprecipitated with MRP-specific Mab (QCRL-1) or an irrelevant IgG_{2a}. Panel B shows total membranes from H69 and H69/AR cells after silver staining. Panel C shows the photoaffinity labeling of H69/AR membranes with increasing concentrations of IACI (from 0 to 4.0 μM). The inset of panel C shows the increase in the intensity of 190 kDa photolabeled protein which was excised and the radiolabel quantified. Panel D shows the photoaffinity-labeled proteins from H69 or H69/AR cells incubated in the absence or presence of excess (0.1−100 μM) noniodinated IACI.

by IACI in H69/AR but not in H69 membranes. When similar membrane samples were photoaffinity labeled by [^{125}I]iodoarylazidoprazosin or [^{3}H]azidopine, shown previously to photolabel P-glycoprotein (*47*), no 190 kDa protein was photoaffinity labeled (results not shown and ref *28*). These results suggest that neither iodoarylazidoprazosin nor azidopine photoaffinity labels the 190 kDa protein in H69/AR membranes. The identity of the 190 kDa protein as the MRP was confirmed by immunoprecipitation of IACI-photolabeled plasma membranes from H69/AR cells with the MRP-specific monoclonal antibody, QCRL-1. Figure 2A shows that the IACI-photolabeled 190 kDa protein can specifically immunoprecipitate with QCRL-1 from H69/AR but not from H69 membranes. Moreover, no IACI photoaffinity-labeled 190 kDa protein was immunoprecipitated with an irrelevant antibody (Figure 2A).

To determine if photolabeling of the 190 kDa protein (or MRP) in membranes from H69/AR cells is due to nonspecific binding to an abundant protein, total membrane proteins from H69 and H69/AR cells were resolved by SDS−PAGE on a 6% Laemmli gel (*41*) and visualized by silver staining. Comparison of H69 and H69/AR proteins did not show significant differences, except for the broad band at ~190 kDa (Figure 2B). Interestingly, the region where MRP photoaffinity labeling is observed, between 113 and 200 kDa (Figure 2A), shows no photoaffinity labeling of some abundantly expressed proteins. High levels of protein expression are seen for both H69 and H69/AR cells between the 113 and 50 kDa molecular mass markers (Figure 2B). This may account for some of the photolabeling of certain abundantly expressed proteins seen below the 113 kDa molecular mass marker. To further confirm the binding specificity of IACI toward the 190 kDa protein, H69/AR membranes were photoaffinity labeled with increasing concentrations (from 0.25 to 4.0 μM) of IACI. The inset of Figure 2C shows that the photoaffinity labeling of the 190 kDa protein is saturable at 4.0 μM drug. Furthermore, the specificity of IACI toward the 190 kDa protein was confirmed by photolabeling in the presence of a molar excess (40−400-fold) of the uniodinated IACI. Lanes d and e of Figure 2D show marked decrease in the extent of photolabeling of the 190 kDa protein in the presence of a molar excess of IACI. The photolabeling which is evident in some lower-molecular mass proteins was not significantly affected with excess uniodinated IACI (Figure 2D).

Inhibition of Photoaffinity Labeling of the MRP. To determine if IACI binds to physiologically relevant site(s) in the MRP, membranes from H69/AR cells were photola-

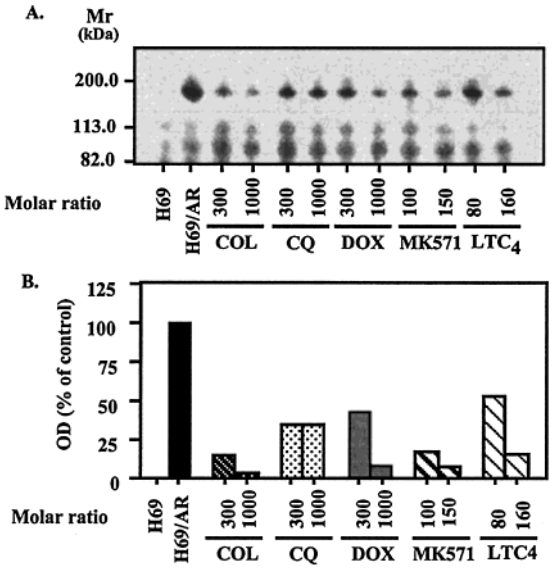

FIGURE 3: Effects of diverse drugs on the photoaffinity labeling of the MRP by IACI. H69 or H69/AR cells were photoaffinity labeled with IACI in the absence or presence of a molar excess (300−1000-fold) of colchicine (COL), chloroquine (CQ), doxorubicin (DOXO), MK571 (100−150-fold), and LTC_4 (80−160-fold). Panel B shows a plot of the relative decrease in the extent of photolabeling of the MRP with IACI in the presence of the drugs listed above.

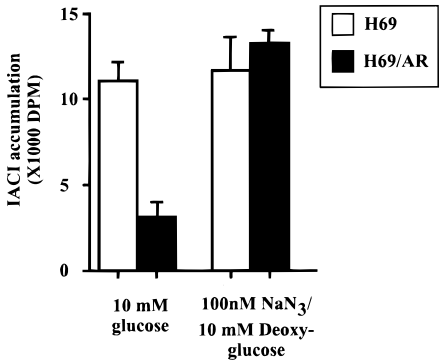

FIGURE 4: Drug accumulation in H69 and H69/AR cells. Cells were preincubated in 10 mM glucose or 2-deoxyglucose and sodium azide prior to the addition of 1 μM IACI. Drug accumulation in cells was assessed 0 and 60 min after the addition of IACI. Cells were lysed, and the amounts of accumulated radiolabel were determined by fluorography. Each value is the mean ± the standard deviation of the two experiments carried out in triplicate.

beled with IACI in the presence of a molar excess of colchicine, chloroquine, doxorubicin, MK571, and LTC_4. The photoaffinity labeling of MRP was inhibited with a 160-fold molar excess of LTC_4 (Figure 3A). Similarly, a molar excess (100−150-fold) of MK571 also led to a dramatic decrease in the extent of photolabeling of the MRP with IACI. Colchicine, chloroquine, and doxorubicin at 1000-fold molar excess were similar to MK571 at 150-fold and LTC_4 at 160-fold, consistent with the higher affinity of MK571 and LTC_4 for the MRP (Figure 4A). The latter results are in accord with the previous findings that LTC_4 is the substrate with the highest affinity for MRP (*11*, *21*, *22*). Together, these results confirm the specificity of IACI toward MRP and suggest that IACI binding to MRP occurs at the same or overlapping site(s) as MK571 and LTC_4.

IACI Accumulation in H69 and H69/AR Cells. Given the results described above, it was of interest to determine if IACI is a substrate for MRP transport function. Figure 4 shows the accumulation of IACI in H69 and H69/AR cells in the presence of 10 mM glucose. H69/AR cells exhibit lower steady-state levels of drug accumulation of IACI than H69 cells (Figure 4). Moreover, preincubation of cells with 10 mM 2-deoxyglucose and 100 nM sodium azide, which depletes ATP levels, increased the level of accumulation of IACI in H69/AR cells to the same level as that of the H69 parental cells (Figure 4). Taken together, these results show that the accumulation of IACI in MRP-expressing cells is ATP-dependent.

Three Peptides of the MRP Are Photoaffinity Labeled by IACI. Several reports on MRP secondary structure and topology have suggested the presence of five N-terminal transmembrane helices (MSD1), followed by an MDR-like core of six duplicated transmembrane domains and an ATP binding site (*16*−*18*). Limited proteolysis of MRP has revealed two trypsin sensitive sites (L1 and L2; see Figure 5B) that connect MSD1 to MSD2 and MSD3, and MSD1 and MSD2 to MSD3 sequences (*48*). The L2 sequence was shown to be more sensitive to trypsin cleavage than the L1 sequence (*48*). Therefore, limited proteolysis of MRP with trypsin showed two polypeptides with molecular masses of 120 and 75−80 kDa containing MSD1, MSD2, and NBD1, and MSD3 and NBD2, respectively (*16*−*18*). However, further digestion with trypsin led to the cleavage of the 120 kDa polypeptide into two smaller peptides (40−60 and 57 kDa) that correspond to MSD1, and MSD2 and NBD1, respectively (*16*−*18*). Taking advantage of the trypsin sensitive sites in the MRP, it was of interest to map IACI photoaffinity-labeled peptides in the MRP. Figure 5A shows the results of subjecting the IACI-photolabeled MRP to mild proteolysis with trypsin and the digested products resolved by SDS−PAGE. Lanes 3 and 4 of Figure 5A show two major photoaffinity-labeled polypeptides that migrate with apparent molecular masses of 111 and 85 kDa. Figure 5C shows Western blots of the same samples as in Figure 5A probed with MRPr1, QCRL-1, and MRPm6 Mabs. The Mabs QCRL-1 and MRPm6 recognized the 85 kDa polypeptide, while MRPr1 recognized the 111 kDa fragment (Figure 5C). These results are consistent with earlier proteolysis of MRP (*16*−*18*) whereby the 85 kDa polypeptide contains the QCRL-1 and MRPm6 epitopes while the 111 kDa polypeptide contains the MRPr1 epitope (*48*). Therefore, the two photoaffinity-labeled polypeptides (111 and 85 kDa) correspond to the MRP sequence containing MSD1, MSD2, and NBD1, and MSD3 and NBD2, respectively. Probing the same nitrocellulose membrane with goat anti-mouse peroxidase second antibody alone did not show any reactive proteins (data not shown). Taken together, these results demonstrate the photoaffinity labeling of two different domains in the MRP.

To determine the number of IACI-photolabeled sites in the MRP, the photoaffinity-labeled MRP was immunopurified with QCRL-1 and subjected to in-gel digestion with increasing concentrations of *S. aureus* V8 protease (1−20 μg/gel slice). Figure 6A shows the resultant proteolytic fragments migrating with apparent molecular masses of 6 and 4 kDa. Similarly, the IACI photoaffinity-labeled MRP was subjected to exhaustive trypsin digestion (see Materials and Methods), and the resulting digest was resolved by HPLC using reverse phase chromatography. Figure 6B shows

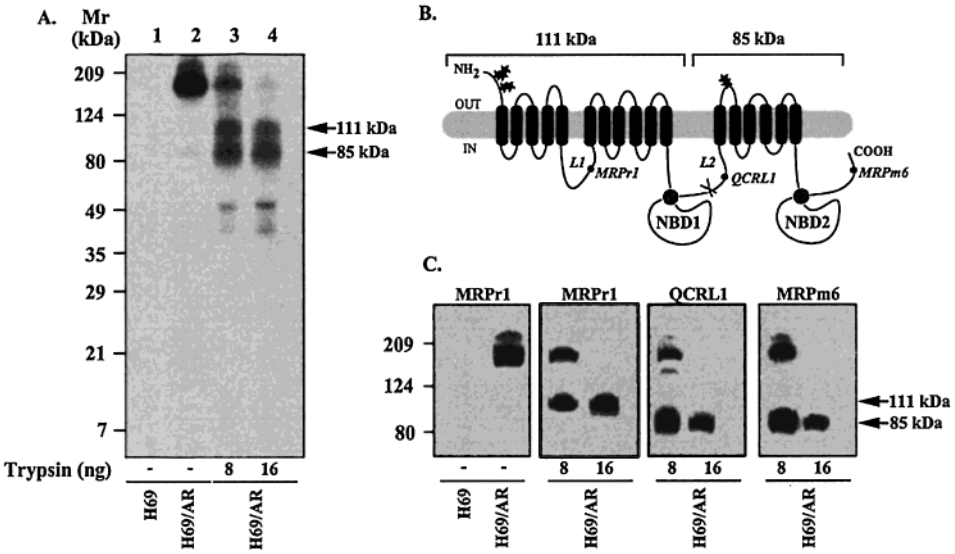

FIGURE 5: Photoaffinity labeling of two large polypeptides of the MRP by IACI. The MRP photoaffinity labeled by IACI was purified from H69/AR membranes and subjected to mild tryptic digestion. The photolabeled, radiolabeled products were split in two halves; one-half was resolved by SDS−PAGE (A), while the second half was resolved by SDS−PAGE and transferred to nitrocellulose for Western blotting (C). Lanes 2−4 of panel A show the signal from the purified IACI-photolabeled MRP incubated in the absence and in the presence of 8 and 16 ng of trypsin, respectively. Panel C shows the Western blot of the IACI-photolabeled MRP tryptic digest probed separately with MRPr1, QCRL-1, and MRPm6 Mabs. Panel B shows a schematic of the predicted MRP topology with the three monoclonal antibody epitopes listed above in the MRP relative to the protease hypersensitive sites (L1 and L2). The nucleotide binding domains (NBD1 and NBD2) and the extracellular glycosylation sites (**) are indicated on the schematic of MRP secondary structure (B).

the eluted IACI-photolabeled, radiolabeled tryptic peptides resolved on a C_{18} reverse phase column with a 0 to 100% acetonitrile gradient. The results in Figure 6B show one minor peak eluting at 60% acetonitrile followed by two major peaks eluting at 65−72% acetonitrile.

To identify the origin of the 4 and 6 kDa IACI-photolabeled peptides relative to the two large photolabeled domains of the MRP, IACI-photolabeled 111 and 85 kDa polypeptides were purified and digested with *S. aureus* V8 protease. Lanes 2 and 3 of Figure 7A show IACI-photolabeled 111 and 85 kDa polypeptides following immunoprecipitation with MRPr1 and MRPm6 Mabs, respectively. Exhaustive digestion of the 111 kDa polypeptide which corresponds to MSD1, MSD2, and NBD1 of the MRP resulted in two photolabeled peptides which migrate with apparent molecular masses of 4 and 6 kDa (Figure 7B). However, digestion of the 85 kDa polypeptide, which corresponds to MSD3 and NBD2 of the MRP, resulted in only one photolabeled peptide of 6 kDa (Figure 7B). Taken together, the results in Figure 7 suggest the presence of three IACI-labeled sites in the MRP.

DISCUSSION

It is now believed that the overexpression of the MRP in tumor cell lines can confer resistance to certain natural product toxins (*23*, *49*). Moreover, MRP-mediated transport of normal cell metabolites has been demonstrated in intact cells and in MRP-enriched membrane vesicles (*11*, *21*−*23*). However, the mechanism of MRP drug binding and transport remains unclear: (i) MRP's broad substrate specificity, (ii) MRP's ability to bind and transport unmodified drugs, (iii) the role of free GSH in MRP drug binding and transport, and (iv) MRP drug binding site(s). In this report, we have used a photoreactive quinoline-based drug (IACI) to examine MRP−drug interactions. Our results show the photoaffinity labeling of a 190 kDa protein by IACI only in drug resistant cells (H69/AR). The identity of the IACI-photolabeled protein, as the MRP, was confirmed by its binding to three MRP-specific monoclonal antibodies (QCRL-1, MRPr1, and MRPm6; *48*). The photolabeling of MRP in enriched membranes from H69/AR cells suggests direct binding between the MRP and unmodified IACI. Moreover, the addition of free GSH (up to 5 mM) did not cause a significant change in MRP photoaffinity labeling (results not shown). With respect to the role of GSH in MRP drug transport, ATP-dependent transport of unmodified vincristine into membrane vesicles was shown only in the presence of GSH (*30*). Thus, although the authors of that study (*30*) did not examine vincristine binding to the MRP, it is likely that drug transport but not drug binding required the presence of free GSH. Alternatively, GSH may be required for the binding and transport of certain classes of drugs. Future experiments will examine the effect of GSH and other MRP substrates on IACI transport in membrane vesicles from MRP-expressing cells. Taken together, these findings demonstrate direct binding between the MRP and the unmodified drug that is unaffected by GSH.

The questions of whether IACI is a relevant substrate for the MRP and whether the photoaffinity labeling of the MRP by IACI occurs at a physiologically relevant site(s) were addressed by drug transport and drug competition experiments. Our transport results show IACI is a substrate for MRP drug efflux as it accumulates less in MRP-expressing cells (H69/AR) than in the parental cells (H69). Furthermore, depletion of ATP levels by preincubating cells with sodium azide and 2-deoxyglucose restored IACI accumulation in H69/AR cells to the same level as in H69 cells. The possibility that differences in IACI accumulation between H69/AR and H69 cells are due to changes or ATP-dependent mechanisms other than the MRP cannot be ruled out

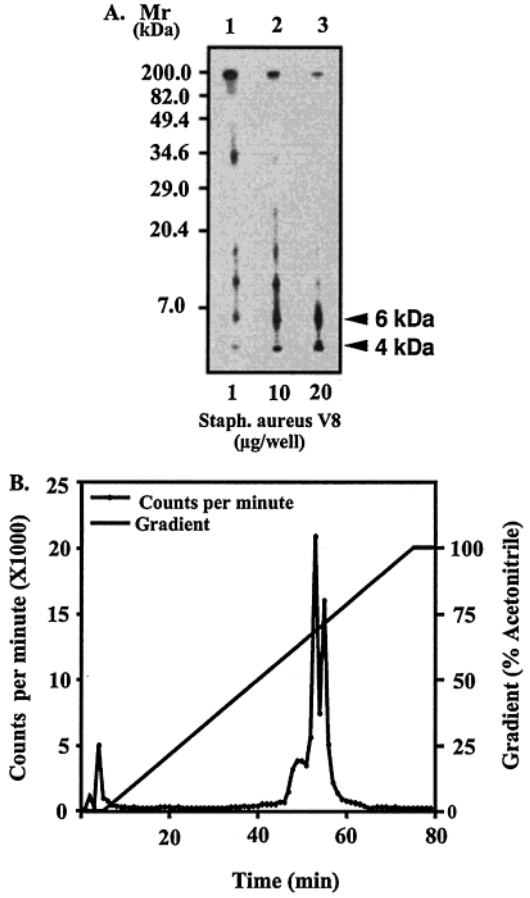

FIGURE 6: Complete proteolytic digestion of the IACI photoaffinity-labeled MRP yields two labeled peptides. The purified MRP photoaffinity labeled with IACI was subjected to complete in-gel or solution digestion. The in-gel-digested MRP products were resolved on 15% acrylamide SDS−PAGE, while the solution-digested products were resolved by reverse phase chromatography. Lanes 1−3 of panel A show an in-gel digestion of the IACI-photolabeled MRP with increasing concentrations of *S. aureus* V8 protease (1−20 μg/well). Panel B shows the separation of MRP photoaffinity-labeled tryptic peptides on a C_{18} reverse phase column using a 0 to 100% acetonitrile gradient. The amount of radiolabel in each eluted fraction was plotted vs time of elution in the gradient. The peak signal at the beginning of the gradient represents the void volume.

completely on the basis of our drug transport data alone. However, along with the photoaffinity labeling results, described in this study, compelling evidence for MRP-mediated transport of IACI exists. The inhibition of MRP photolabeling by IACI with a molar excess of LTC_4 indicates that IACI binds to the MRP at a physiologically relevant site. Although little is known about MRP drug binding domain(s), we speculate that IACI binds to the same domain (or an overlapping one) as that of MK571 or LTC_4. Alternatively, IACI may bind at another site that is allosterically linked to the LTC_4 binding domain. In a recent study by Stride et al. (*50*), it was shown that substitution of the carboxyl third of the human MRP with that of mouse mrp sequences modulated MRP specificity to the anthracycline doxorubicin while LTC_4 transport was unaffected, thus confirming further the notion of more than one drug binding site in the MRP. In addition, support for multiple drug binding sites in the MRP comes from studies with another broad spectrum transporter (P-gp1) which is thought to encode three drug binding sites (*51*).

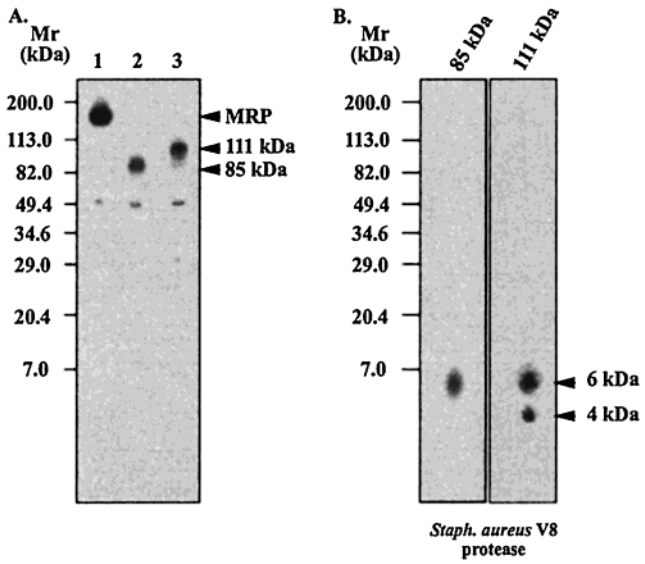

FIGURE 7: Proteolytic cleavage of the immunopurified IACI-photolabeled N- and C-halves of MRP. MRP-enriched membranes were photolabeled with IACI and subjected to mild tryptic cleavage. Lanes 1−3 of panel A show immunoprecipitation of native and trypsin-digested MRP with MRPm6 and MRPr1 Mabs, respectively. Panel B shows complete digestion of immunopurified IACI-photolabeled 111 and 85 kDa polypeptides with *S. aureus* V8 protease. The digested fragments were resolved on the Fairbanks gel system. The apparent molecular masses of standard proteins are indicated to the left of the gels.

Studies of MRP topology are in agreement with the two "6+6" transmembrane helices (or MSD2 and MSD3) and two NBDs characteristic of many ABC transporters, in addition to the hydrophobic N-terminal domain predicted to encode five transmembrane helices (MSD1) (*17*, *18*). A previous limited proteolysis study (*48*) showed that the MRP contains two hypersensitive regions (L1 and L2) connecting MSD1 to MS2 and MSD3, and MSD1 and MSD2 to MSD3, respectively. In this study, we took advantage of the protease hypersensitive regions in MRP linker domains together with the positions of three monoclonal antibodies with known epitope sequences in the MRP to identify the photoaffinity labeling domains in the MRP. Mild trypsin digestion of IACI-photolabeled MRP produced two large photolabeled polypeptides with apparent molecular masses of ~111 and ~85 kDa on SDS−PAGE. On the basis of the locations of MRPr1, QCRL-1, and MRPm6 epitopes (at ^{238}GSDLWSLNKE^{247}, ^{918}SSYSGD^{924}, and ^{1511}PSDLLQQRGL^{1520}, respectively; *48*) relative to one of the trypsin hypersensitive sites in the MRP linker domain (L2) (*17*, *48*), the 111 kDa polypeptide corresponds to the N-terminal MSD1 and MSD2 and NBD1. Similarly, the 85 kDa polypeptide should encode MSD3 and NBD2 as it reacted only with QCRL-1 and MRPm6 Mabs (see Figure 5). Exhaustive digestion of the IACI-photolabeled MRP with V8 protease revealed two photolabeled peptides with apparent molecular masses of ~6 and ~4 kDa. However, digestion of purified 111 and 85 kDa polypeptides with V8 protease revealed three IACI-photolabeled peptides, two (6 and 4 kDa) from the 111 kDa polypeptide and one (6 kDa) from the 85 kDa polypeptide. Although the possibility that the 6 kDa peptide, from the 111 kDa fragment, results from incomplete digestion cannot be entirely ruled out, it is unlikely given the exhaustive nature of our digestion conditions. Furthermore, exhaustive digestion of the IACI-

labeled MRP with trypsin showed two major and one minor peak (Figure 6B), consistent with a total of three IACI-photolabeled peptides. The photoaffinity labeling of MRP at multiple sites is consistent with that observed with another membrane transporter protein, P-gp1 (*32*). The exact amino acid sequence of P-gp1 drug binding sites is presently not known; however, several reports support the role of transmembrane helices 5 and 6 and 11 and 12 in drug binding and transport (*33*). The photoaffinity labeling of three peptides in the MRP with IACI suggests MRP drug binding may involve three domains. Given the hydrophobic nature of MRP substrates and our knowledge of P-gp1 drug binding domains, it is tempting to speculate that the three IACI-photolabeled peptides correspond to the three membrane-spanning domains (MSD1−3) in the MRP.

Although it is likely that the drug binding domains in the MRP and the photoaffinity-labeled sites are different, earlier studies with P-gp1 have shown these sites to be the same or to overlap (*32*, *33*). Photoaffinity labeling studies of P-gp1 are in agreement with other molecular approaches. Indeed, results from the photoaffinity labeling studies were used as a starting point for mutational analyses of P-gp1 sequences. Furthermore, results from a recent study aimed at localizing MRP specificity domains toward anthracyclines suggested a role for the carboxyl third of the MRP (*50*). The latter findings are consistent with our results in this report which show the photoaffinity labeling of the carboxyl third of MRP (MSD3 and NBD2) (*50*).

A molar excess of colchicine and doxorubicin also caused a significant decrease in the extent of MRP photoaffinity labeling by IACI. These findings are interesting since earlier analysis of the cross resistance of MRP-expressing cells showed only low levels of cross resistance to colchicine (*52*). Inhibition of photoaffinity labeling of IACI with MK571 and CQ is less surprising as both drugs share the quinoline moiety. The LTD_4 receptor antagonist, MK571 (*36*), was recently shown to inhibit LTC_4 and *S*-(*p*-azidophenylacyl)-glutathione labeling of the MRP (*11*, *46*) and to reverse MRP-mediated MDR (*35*). Indeed, several quinoline-based drugs have been reported to interact directly and specifically with the MRP (*27*, *28*, *53*), hence establishing this group as another class of compounds that interact with MRP. Collectively, these findings are important as many therapeutically important drugs are quinoline-based drugs (*54*). For example, quinoline-based drugs are extensively used in the treatment of parasitic infections such as malaria (*55*, *56*), and resistance to these drugs has rendered this first-choice drug treatment ineffective (*55*, *56*). Given these findings, we speculate about an MRP-like mechanism responsible for resistance in this parasite.

In conclusion, there is increasing evidence that the MRP mediates the transport of structurally diverse drugs through direct binding. Although several studies have demonstrated direct binding between the MRP and LTC_4 using a photoaffinity labeling assay, photoaffinity labeling of the MRP by [^{3}H]LTC_4 was inefficient, requiring large amounts of membrane (200 μg/sample) and extremely long exposure times (more than 4 weeks in our hands). By contrast, photoaffinity labeling of the MRP by IACI was done using 20 μg of membranes/sample, and exposure for 2−12 h showed a strong signal for MRP. The availability of a photoactive radioiodinated drug that binds specifically to the MRP should facilitate future analysis of MRP−drug interactions. The photoaffinity labeling of the MRP at multiple sites which map to two domains in the MRP is consistent with protein−drug interactions seen with other members of the ABC family of drug transporters, such as P-gp1. Finally, we show that IACI binding to the MRP is inhibited by known substrates of MRP, LTC_4, and other natural product drugs. We speculate that IACI binds to the same domain (or an overlapping domain) as that of LTC_4 or MK571. Work is in progress to determine if IACI photoaffinity labels the same or different sequences as MK571 and LTC_4.

ACKNOWLEDGMENT

We thank Joel Karwatsky for his careful reading of the manuscript.

REFERENCES

1. Gottesman, M. M., and Pastan, I. (1993) *Annu. Rev. Biochem. 62*, 385−427.
2. Endicott, J. A., and Ling, V. (1989) *Annu. Rev. Biochem. 58*, 137−171.
3. Cole, S. P., and Deeley, R. G. (1996) *Cancer Treat. Res. 87*, 39−62.
4. Ueda, K., Cardarelli, C., Gottesman, M. M., and Pastan, I. (1987) *Proc. Natl. Acad. Sci. U.S.A. 84*, 3004−3008.
5. Grant, C. E., Valdimarsson, G., Hipfner, D. R., Almquist, K. C., Cole, S. P., and Deeley, R. G. (1994) *Cancer Res. 54*, 357−361.
6. Schinkel, A. H., Smit, J. J. M., van Tellingen, O., Beijnen, J. H., Wagenaar, E., van Deemter, L., Mol, C. A. A. M., var der Valk, M. A., Robanus-Maandag, E. C., te Riele, H. P. J., Berns, A. J. M., and Borst, P. (1994) *Cell 77*, 491−502.
7. Lorico, A., Rappa, G., Flavell, R. A., and Sartorelli, A. C. (1996) *Cancer Res. 56*, 5351−5355.
8. Wijnholds, J., Evers, R., van, L. M., Mol, C., Zaman, G., Mayer, U., Beijnen, J., van, d. V. M., Krimpenfort, P., and Borst, P. (1997) *Nat. Med. 3*, 1275−1279.
9. Ruetz, S., and Gros, P. (1994) *Cell 77*, 1071−1081.
10. Raggers, R. J., van Helvoort, A., Evers, R., and van Meer G. (1999) *J. Cell Sci. 112*, 415−422.
11. Leier, I., Jedlitschky, G., Buchholz, U., Cole, S. P., Deeley, R. G., and Keppler, D. (1994) *J. Biol. Chem. 269*, 27807−27810.
12. Lorico, A., Rappa, G., Finch, R. A., Yang, D., Flavell, R. A., and Sartorelli, A. C. (1997) *Cancer Res. 57*, 5238−5242.
13. Rappa, G., Lorico, A., Flavell, R. A., and Sartorelli, A. C. (1997) *Cancer Res. 57*, 5232−5237.
14. Higgins, C. F. (1995) *Cell 82*, 693−696.
15. Stride, B., Grant, C., Loe, D., Hipfner, D., Cole, S., and Deeley, R. (1997) *Mol. Pharmacol. 52*, 344−353.
16. Bakos, E., Hegedus, T., Hollo, Z., Welker, E., Tusnady, G. E., Zaman, G. J., Flens, M. J., Varadi, A., and Sarkadi, B. (1996) *J. Biol. Chem. 271*, 12322−12326.
17. Hipfner, D. R., Almquist, K. C., Leslie, E. M., Gerlach, J. H., Grant, C. E., Deeley, R. G., and Cole, S. P. C. (1997) *J. Biol. Chem. 272*, 23623−23630.
18. Kast, C., and Gros, P. (1997) *J. Biol. Chem. 272*, 26479−26487.
19. Gao, M., Yamazaki, M., Loe, D., Westlake, C., Grant, C., Cole, S., and Deeley, R. (1998) *J. Biol. Chem. 273*, 10733−10740.
20. Bakos, E., Evers, R., Szakacs, G., Tusnady, G., Welker, E., Szabo, K., de, H. M., van Deemter, L., Borst, P., Varadi, A., and Sarkadi, B. (1998) *J. Biol. Chem. 273*, 32167−32175.
21. Jedlitschky, G., Leier, I., Buchholz, U., Barnouin, K., Kurz, G., and Keppler, D. (1996) *Cancer Res. 56*, 988−994.
22. Loe, D. W., Almquist, K. C., Cole, S. P., and Deeley, R. G. (1996) *J. Biol. Chem. 271*, 9683−9689.
23. Zaman, G. J. R., Flens, M. J., Vanleusden, M. R., Dehaas, M., Mulder, H. S., Lankelma, J., Pinedo, H. M., Scheper, R. J., Baas, F., Broxterman, H. J., and Borst, P. (1994) *Proc. Natl. Acad. Sci. U.S.A. 91*, 8822−8826.

24. Ishikawa, T. (1992) *Trends Biochem. Sci. 17*, 463−468.
25. Jansen, P. L. M., and Oude Elferink, R. P. J. (1993) in *Defective Hepatic Anion Secretion in Mutant TR-Rats*, Raven, New York.
26. Zaman, G. J. R., Lankelma, J., Tellingen, O. V., Beijnen, J., Dekker, H., Paulusma, C., Elferink, R. P. J. O., Baas, F., and Borst, P. (1995) *Proc. Natl. Acad. Sci. U.S.A. 92*, 7690−7694.
27. Vezmar, M., and Georges, E. (1988) *Biochem. Pharmacol. 56*, 733−742.
28. Vezmar, M., Deady, L. W., Tilley, L., and Georges, E. (1997) *Biochem. Biophys. Res. Commun. 241*, 104−111.
29. Nakamura, T., Oka, M., Aizawa, K., Soda, H., Fukuda, M., Terashi, K., Ikeda, K., Mizuta, Y., Noguchi, Y., Kimura, Y., Tsuruo, T., and Kohno, S. (1999) *Biochem. Biophys. Res. Commun. 255*, 618−624.
30. Loe, D. W., Almquist, K. C., Deeley, R. G., and Cole, S. P. (1996) *J. Biol. Chem. 271*, 9675−9682.
31. Chowdry, V., and Westheimer, F. H. (1979) *Annu. Rev. Biochem. 48*, 293−325.
32. Greenberger, L. M. (1993) *J. Biol. Chem. 268*, 11417−11425.
33. Loo, T., and Clarke, D. (1998) *Methods Enzymol. 292*, 480−492.
34. Cole, S., and Deeley, R. (1998) *BioEssays 20*, 931−940.
35. Gekeler, V., Ise, W., Sanders, K. H., Ulrich, W. R., and Beck, J. (1995) *Biochem. Biophys. Res. Commun. 208*, 345−352.
36. Jones, T. R., Zamboni, R., Belley, M., Champion, E., Charette, L., Ford-Hutchison, A. W., Frenette, R., Gauthier, J.-Y., Leger, S., Masson, P., McFarlane, C. S., Piechuta, H., Rokach, J., Williams, H., Young, R. N., DeHaven, R. N., and Pong, S. S. (1989) *Can. J. Physiol. Pharmacol. 67*, 17−28.
37. Lin, P. H., Selinfreund, R., Wakshull, E., and Wharton, W. (1987) *Biochemistry 26*, 731−736.
38. Lowry, O. H., Rosebrough, N. J., Farr, A. L., and Randall, R. J. (1951) *J. Biol. Chem. 193*, 265−275.
39. Desneves, J., Thorn, G., Berman, A., Galatis, D., La Greca, N., Sinding, J., Foley, M., Deady, L. W., Cowman, A. F., and Tilley, L. (1996) *Mol. Biochem. Parasitol. 82*, 181−194.
40. Fairbanks, G., Steck, T. L., and Wallach, D. F. H. (1971) *Biochemistry 10*, 2606−2617.
41. Laemmli, U. K. (1970) *Nature 227*, 680−685.
42. Cleveland, D. W., Fischer, S. G., Kirschner, M. W., and Laemmli, U. K. (1977) *J. Biol. Chem. 252*, 1102−1106.
43. Georges, E., Zhang, J.-T., and Ling, V. (1991) *J. Cell. Physiol. 148*, 479−484.
44. Liu, Z., Lheureux, F., Pouliot, J.-F., Heckel, A., Bamberger, U., and Georges, E. (1996) *Mol. Pharmacol. 50*, 482−492.
45. Paul, S., Breuninger, L. M., Tew, K. D., Shen, H., and Kruh, G. D. (1996) *Proc. Natl. Acad. Sci. U.S.A. 93*, 6929−6934.
46. Leier, I., Jedlitschky, G., Buchholz, U., and Keppler, D. (1994) *Eur. J. Biochem. 220*, 599−606.
47. Safa, A. (1998) *Methods Enzymol. 292*, 289−307.
48. Hipfner, D., Almquist, K., Stride, B., Deeley, R., and Cole, S. (1996) *Cancer Res. 56*, 3307−3314.
49. Almquist, K. C., Loe, D. W., Hipfner, D. R., Mackie, J. E., Cole, S. P., and Deeley, R. G. (1995) *Cancer Res. 55*, 102−110.
50. Stride, B. D., Cole, S. P. C., and Deeley, R. G. (1999) *J. Biol. Chem. 274*, 22877−22883.
51. Shapiro, A., Fox, K., Lam, P., and Ling, V. (1999) *Eur. J. Biochem. 259*, 841−850.
52. Cole, S. P., Sparks, K. E., Fraser, K., Loe, D. W., Grant, C. E., Wilson, G. M., and Deeley, R. G. (1994) *Cancer Res. 54*, 5902−5910.
53. Priebe, W., Krawczyk, M., Kuo, M. T., Yamane, Y., Savaraj, N., and Ishikawa, T. (1997) *Proc. Am. Assoc. Cancer Res. 38*, 440.
54. Baba, A., Kawamura, N., Makino, H., Ohta, Y., Taketomi, S., and Sohda, T. (1996) *J. Med. Chem. 39*, 5176−5182.
55. Foley, M., and Tilley, L. (1997) *Int. J. Parasitol. 27*, 231−240.
56. Foley, M., and Tilley, L. (1998) *Pharmacol. Ther. 79*, 55−87.

BI9922188